Sánchez-Muñoz, EJ.; Berjano, E.; González-Suárez, A. (2022). Computer simulations of consecutive radiofrequency pulses applied at the same point during cardiac catheter ablation: Implications for lesion size and risk of overheating. Computer Methods and Programs in Biomedicine. 220:1-9. https://doi.org/10.1016/j.cmpb.2022.106817

Computer simulations of consecutive radiofrequency pulses applied at the same point during cardiac catheter ablation:

Implications for lesion size and risk of overheating

Eugenio J Sánchez-Muñoz[1], Enrique Berjano[2], Ana González-Suárez[3,4]

From [1] Universidad Internacional de Valencia (VIU), Valencia, Spain, [2]BioMIT, Department of Electronic Engineering, Universitat Politècnica de València, Valencia, Spain, [3] Electrical and Electronic Engineering, National University of Ireland Galway, Ireland, [4] Translational Medical Device Lab, National University of Ireland Galway, Ireland

Corresponding author: Dr. Ana González-Suárez, Translational Medical Device Lab, 2nd Floor, Lambe Translational Research Facility, University College Hospital Galway, Ireland.
Email: ana.gonzalezsuarez@nuigalway.ie

Funding details: Grant RTI2018-094357-B-C21 funded by MCIN/AEI/10.13039/501100011033.

Declaration of interest: The authors have no conflicts of interest or financial disclosures to make relevant to this submission.

Running head: Effect of the interval between consecutive RF pulses
Data availability: The data underlying this article will be shared on reasonable request to the corresponding author.

Abstract

Background and objectives: To study temperature distribution and lesion size during two repeated radiofrequency (RF) pulses applied at the same point in the context of RF cardiac ablation (RFCA).

Methods: An *in-silico* RFCA model accounting for reversible and irreversible changes in myocardium electrical properties due to RF-induced heating. Arrhenius damage model to estimate lesion size during the application of two 20 W pulses at intervals (INT) of from 5 to 70 s. We considered two pulse durations: 20 s and 30 s.

Results: INT has a significant effect on lesion size and maximum tissue temperature (TMAX). The shorter the INT the greater the increase in lesion size after the second pulse but also the greater the TMAX. If the second pulse is applied almost immediately (INT=5 s), depth increases 1.4 mm and 1.5 mm for pulses of 20 s and 30 s, respectively. If INT is longer than 30 s it increases 1.1 mm and 1.3 mm for pulses of 20 s and 30 s, respectively. While a single 20 s pulse causes T_{MAX}=79 ºC, a second pulse produces values of from 92 and 96 ºC (the higher the temperature the shorter the INT). For 30 s pulses, T_{MAX}=93 ºC for a single pulse, and varied from 98 to 104 ºC for a second pulse.

Conclusions: Applying a second RF pulse at the same ablation site increases lesion depth by 1–1.5 mm more than a single pulse and could lead to higher temperatures (up to 17 ºC). Both lesion depth and maximum tissue temperature increased at shorter inter-pulse intervals, which could cause clinical complications from overheating such as steam pops.

Keywords: *In-silico* study; lesion overlapping; repeated application; RF ablation.

1. Introduction

Radiofrequency (RF) cardiac ablation (RFCA) is a minimally invasive procedure to destroy the group of cardiac cells that cause arrhythmia. Posterior wall isolation can be conducted by RFCA to cure atrial fibrillation (AF) by creating complete lines based on a sequence of multiple point lesions created by the active electrode on the catheter tip. While these lesions should be as close as possible to each other to achieve contiguous lines and avoid conduction gaps (3–4 mm distance between applications [1]), an attempt is always made to avoid applying RF power on a previously ablated site for safety reasons. In the treatment of ventricular tachycardia, repeated RF pulses at adjacent sites may be required for ablation of extended arrhythmogenic areas [2]. Although repeated applications are suspected of leading to overheating and complications, the electrical and thermal phenomena associated with the repeated application of RF pulses are not yet fully understood.

There is hardly any experimental or clinical data describing the characteristics of the thermal lesions created on a previously ablated point. Ring *et al* [3] addressed this issue using an *in vitro* heart model. Their power setting was different from the one currently used in AF ablation since the ablations were not interrupted, despite impedance rises (sudden drops in electrical current). These were frequently associated with a marked disruption of the endocardial surface with char and coagulum formation [3]. These authors found that after an impedance rise, subsequent applications of radiofrequency (RF) power on the same site resulted in a progressively shorter time to impedance rise. These findings have possibly spread the idea that overheating will occur more quickly if RF power is applied on an already ablated site although a detailed physical explanation for this behavior has not yet been provided. Ring *et al* suggested that since the integrity of the RF catheter was unchanged after each RF pulse, the cause would lie in

predominant alterations in tissue impedance.

Our specific hypothesis is that the electro-thermal behavior of the tissue during a second RF pulse is conditioned by the presence of a more conductive substrate due to reversible and irreversible changes in electrical conductivity (σ) of the previously ablated myocardium. Reversible change only depends on the temperature at a given time and increases with temperature by ~1.5%/ºC up to 100 ºC. This implies that the tissue is more conductive during heating but returns to its initial value when the temperature returns to baseline. In contrast, irreversible change takes into account the degree of thermal damage (i.e. coagulative necrosis) reached in the tissue after the first pulse [4], so that electrical conductivity no longer returns to the initial value. Our objective was to use *in-silico* modeling to study temperature distribution and lesion size during two repeated applications of RF power on the same site, determine the role of the interval between RF pulses, and provide a physical explanation of the phenomena involved. *In-silico* modeling has demonstrated to be a fine tool to study RF ablation in different medical fields, such as tumor [5] and cardiac ablation [6].

2. Methods

2.1. Modeling of electrical conductivity of the myocardium

Although there are still no specific experimental data on changes in electrical conductivity (σ) of the myocardium just after thermal ablation, reasonable assumptions can be made in two complementary ways: 1) available data from other ablated tissues, and 2) data on infarcted myocardium. Pop *et al* [4] studied the reversible and irreversible changes in kidney σ associated with RF-induced heating. They found that σ increased irreversibly by ~50% after heating up to 70 ºC (above this temperature, desiccation from tissue shrinkage confused the measurements).

This irreversible change was associated with structural changes. While the fresh samples of kidney were initially reddish-pink in color, moist and soft, after heating at ablative levels (64−71 ºC) and a subsequent cooling period (>10 min) the tissue became white and had a slightly harder texture (samples treated at 78 ºC were yellowish-brown, shrunken and very hard). Microscopically, samples heated at >60 ºC were generally characterized by cellular disintegration with an interstitium full of products from cellular organelle dissolution. There is no reason to think that the relationship between σ changes and cellular alterations reported by Pop *et al* are different to those in the myocardium. In fact, the appearance of nonviable myocardium after RF ablation is also pale, and in histological terms the cellular membranes are either absent or severely distorted and discontinuous [7]. This assumption is also in agreement with that observed in clinical practice, where the impedance returns to values lower than the initial values after the application of the RF [8].

Secondly, some experimental studies have shown that healed infarcted myocardium (which is made up mainly of fibroblast and collagen and has a very low proportion of surviving cardiac cells) is more conductive than healthy myocardium. For instance, Salazar *et al* [9] reported a higher mean value of σ at 316 kHz for infarcted myocardium (0.8 S/m) than for healthy myocardium (0.55 S/m), i.e. 45% higher. Likewise, Schwartzman *et al* [10] reported a value of ~0.33 S/m for densely infarcted myocardium (both at 100 kHz and 1 MHz), and values of 0.18 S/m and 0.31 S/m for healthy myocardium at 100 kHz and 1 MHz, respectively. Interpolating between 100 kHz and 1 MHz for healthy myocardium results in a value of 0.24 S/m (very similar to that reported in the ITIS database at 500 kHz, 0.28 S/m) [11], i.e. 38% higher. Since tissue conductivity is closely related to the presence of cell membranes, which prevent the passage of

electric current, especially at low frequencies, the values reported in these two studies are consistent with the lower cellular content of the infarcted myocardium.

Following the same reasoning, since RF-induced coagulative necrosis occurred during RFCA implies cell membrane rupturing [7], ablated myocardium should have a higher value of σ than the non-ablated myocardium, which preserves cell membranes intact. In brief, until specific experimental data are available, it seems reasonable to assume that the ablated myocardium is more conductive than intact tissue and that this increase could be around 50%, i.e. an increase of $\times 1.5$.

In our study, the reversible and irreversible changes of σ were mathematically modeled as described in [12]. Reversible change, i.e. associated exclusively with temperature, was modeled using a piecewise function characterized by an increase of +1.5%/ºC up to 100 ºC, followed by a reduction of two orders of magnitude between 100 and 105 ºC, with a constant value thereafter. This reduction enables modeling the tissue desiccation associated with vaporization (water loss). On the other hand, the irreversible change was modeled by assuming that $\sigma_{non\text{-}ablated}$ tends towards a new value ($\sigma_{ablated}$) as the ablation progresses. We considered $\sigma_{non\text{-}ablated}$ = 0.281 S/m [11] and $\sigma_{ablated}$ = 0.4215 S/m, i.e. 50% higher, as justified above. To model the change from $\sigma_{non\text{-}ablated}$ to $\sigma_{ablated}$, we used an Arrhenius model as proposed by Pop *et al* [4], which determines the first-order kinetic rate for the irreversible change in σ. The parameter Ω_σ represents the expected fraction of cells unaffected by irreversible change, and is computed as follows:

$$\Omega_\sigma(T,t) = A_\sigma \int_0^t e^{-\frac{\Delta E_\sigma}{R \cdot T(\tau)}} d\tau \qquad (1)$$

where A_σ is the frequency factor (6×10^{34} s^{-1}), ΔE_σ is the activation energy for the irreversible reaction (2.38×10^5 J/mol), R is the universal gas constant (8.314 J/mol·K) and $T(\tau)$ is the absolute

temperature (K) as a function of time. The values of A_σ and ΔE_σ were taken from [4] and were those of *ex vivo* kidney tissue since none are yet available for myocardium. The parameter Ω_σ (associated with irreversible change) was combined with the piecewise function used to model reversible changes) to obtain the following full expression for changes of σ, which is shown in Fig. 1:

$$\sigma(T,\Omega_\sigma) = [\sigma_{non-ablated} + (\sigma_{ablated} - \sigma_{non-ablated})\cdot(1 - e^{-\Omega_\sigma})]\cdot e^{0.015(T-T_{ref})} \quad (2)$$

2.2. Description of the model

Figure 2A shows the geometry of the model, which consisted of a myocardium fragment on which an RF catheter is perpendicularly placed. Blood is also included around the catheter. The catheter tip has an electrode of 8 Fr diameter and 3.5 mm long. We modeled an irrigated electrode as used in RFCA of AF (see section 2.3 to more details). The perpendicular catheter allowed the physical situation to be fully represented by a 2D model with axial symmetry. The electrode was assumed to be inserted initially to 0.5 mm, which represents a similar range to that obtained from a mechanical model [13] for the recommended contact forces for ablation of the posterior wall of the left atrium (5–20 g) [14]. We additionally assessed the effect of changing this value to 0.25 and 0.75 mm. We modeled two consecutive pulses of 20 W (with two durations, 20 and 30 s). The power value used in the simulations was reduced by 20% since the model did not include the entire torso (i.e. 16 W), i.e. we used a limited domain which consists of a fragment of the region of interest around the target area [15]. The interval between RF pulses (t_{INT}) varied from 5 to 70 s, during which RF power was cut off. The simulations were extended

90 s after the second pulse to take into account the extra growth in lesion size due to thermal latency [16].

The computer model was based on a coupled electric-thermal problem which was solved numerically using the Finite Element Method (FEM) with COMSOL Multiphysics software (COMSOL, Burlington, MA, USA). The governing equation for the thermal problem was the Bioheat Equation [17]:

$$\rho c \frac{\partial T}{\partial t} = \nabla \cdot (k \nabla T) + Q_{RF} + Q_p + Q_{met} \quad (3)$$

where ρ is density (kg/m^3), c specific heat (J/kg·K), T temperature (ºC), t time (s), k thermal conductivity (W/m·K), Q_{RF} the heat source caused by RF power (W/m^3), Q_p the heat loss caused by blood perfusion (W/m^3) and Q_m the metabolic heat generation (W/m^3). Both Q_m and Q_p were ignored as these terms are negligible compared to the others [17]. A quasi-static approximation was employed for the electrical problem. The electrical field $\boldsymbol{E}$ distribution was obtained from

$$\boldsymbol{E} = -\nabla \Phi \quad (4)$$

Φ being voltage, which was obtained from:

$$\nabla \cdot (\sigma(T) \nabla \Phi) = 0 \quad (5)$$

σ being electrical conductivity, which varied as temperature and irreversible changes as stated in Eq. (2). The distributed heat source q was then obtained as:

$$Q_{RF} = \sigma |\boldsymbol{E}|^2 \quad (6)$$

In order to model the vaporization in the myocardium, Eq. (3) was written as a balance of enthalpy changes instead of the energy changes proposed in [18]:

$$\frac{\partial h_t}{\partial t} = \nabla (k \nabla T) + Q_{RF} \quad (7)$$

where h_t is the tissue enthalpy per unit volume. This value can be determined by assessing the

amount of energy deposited in the tissue when its temperature is raised from 37 °C to values above 100 °C. According to [18], enthalpy per unit volume is:

$$h_t = \begin{cases} \rho_h c_h (T - 37), & 37 \leq T \leq 99\ ℃ \\ \rho_h c_h (99 - 37) + H_t \cdot \frac{(T-99)}{(100-99)}, & 99 < T \leq 100\ ℃ \\ \rho_h c_h (99 - 37) + H_t + \rho_{dh} c_{dh} (T - 100), & T > 100\ ℃ \end{cases} \quad (8)$$

where the subscript *h* refers to the properties of the hydrated tissue (i.e. before reaching 99 ºC), the subscript *dh* refers to those of the dehydrated tissue, and H_t is the tissue vaporization latent heat. The partial derivative of the enthalpy in Eq. (3) can be therefore expressed as:

$$\frac{\partial h_t}{\partial t} = \begin{cases} \rho_h c_h \frac{\partial T}{\partial t}, & 37 \leq T \leq 99\ ℃ \\ \frac{H_t}{\Delta T} \cdot \frac{\partial T}{\partial t}, & 99 < T \leq 100\ ℃ \\ \rho_{dh} c_{dh} \frac{\partial T}{\partial t}, & T > 100\ ℃ \end{cases} \quad (9)$$

where ΔT = 1 ºC. Apart from the electrical conductivity of the myocardium (which was explained in detail in section 2.1), the rest tissue properties were taken from the IT'IS Foundation database [11], while the ablation catheter properties were taken from Perez *et al* [19].

Figures 2B and 2C show the electrical and thermal boundary conditions, respectively. The initial temperature was 37 ºC. The electrical power applied at the active electrode P_E was set at 16 W, which corresponds to 20 W in clinics [15]. All the outer surfaces of the model were set to 0 V (Dirichlet boundary condition) except that on the symmetry axis, which was fixed at zero electric current (Neumann boundary condition). Likewise, a null thermal flux was set on the symmetry axis and a constant temperature of 37 ºC was fixed on the outer surfaces. The effect of blood circulating inside the cardiac chamber was modeled by thermal convection coefficients at the electrode–blood (h_E) and the tissue–blood (h_T) interfaces, considering electrical conductivity of blood independently of temperature (as in Method 2 in [20]). Each coefficient was calculated under conditions of low blood flow (8.5 cm/s) using the equations described in detail in [20]. The

results were h_E = 3346 W/m^2·K and h_T = 610 W/m^2·K. These values mimic ablation sites with low local blood flow (~10 cm/s), as in patients with chronic atrial fibrillation and dilated atria [21]. Electrode irrigation was modeled using a 'reduced model' as described in [22], which consists of fixing a temperature at 45 ºC only in the cylindrical zone of the electrode tip, leaving the semispherical tip free. We verified that varying this value in the range between 25 and 45 ºC (values reported in experimental studies for the temperature measured in the irrigated electrode) barely affects the results. The 'reduced model' avoids solving the fluid dynamics problem by setting a constant temperature at the electrode tip. This approach is suitable for predicting lesion depth and maximum width (D and MW in Fig. 2A) and maximum tissue temperature, although it tends to overestimate the lesion surface width in comparison with models including the fluid dynamics problem.

2.3. Assessment of the thermal lesion and overheating

Lesion sizes were quantified using depth (D) and maximum width (MW), as shown in Fig. 2A. Although the 50 ºC isotherm is usually considered to compute the irreversible myocardial damage due to RFCA ablation, our study required the use of a function that not only depended on temperature but also on exposure time, since we wanted to analyze cumulative lesion growth, i.e. also taking into account the time when RF power is not active (interval between pulses and RF-post period). The contour of the thermal lesion was thus defined by means of the Arrhenius Equation, which establishes a relationship between the rate of thermal damage accumulation and the temperature, defining the degree of tissue damage:

$$\Omega(T,t) = A\int_0^t e^{-\frac{\Delta E}{R\cdot T(\tau)}} d\tau \qquad (10)$$

where A is the frequency factor (7.39×10^{39} s^{-1}) and ΔE is the activation energy (2.557×10^{5} J/mol) [16]. We considered $\Omega = 1$ as the thermal lesion contour, which represents 63% of dead cells. Note that although thermal damage and irreversible change of σ had the same mathematical formulation they used different values for the model parameters (A frequency factor and ΔE activation energy). The maximum temperature reached in the myocardium (T_{MAX}) was analyzed, since values near to 100 ºC are associated with overheating and possible steam pops.

2.4. Model verification and validation

Verification was done by checking that the computational model (i.e. the result of considering a limited domain as well as discretizing in time and space the mathematical equations to be solved) represents the numerical model of the event with sufficient accuracy [23]. At this regard, mesh size (especially around the active electrode), model dimensions (parameter S in Fig. 2A), and time-step were checked by means of a convergence test using the depth of lesion (D) as a control parameter and differences less than 0.1 mm as a convergence criterion. The finest mesh size was 0.3 mm, S was 40 mm, and the time-step was adaptive during the simulation, with a value of 0.01 s around the transitions (beginning and end of the RF pulses).

About model validation, i.e. the process of determining if a mathematical model of a physical event represents the actual physical event with sufficient accuracy [23], we have to emphasize that we used a numerical model broadly used in past modeling studies and validated in different occasions (such as in [15]), providing prediction errors around 3–7 ºC and 1–2 mm for tissue temperature and lesion size, respectively [6]. In fact, no new features were incorporated in our study in terms of geometry, governing equations, boundary conditions and output variables. So, the model was used to study by simulation the effect of applying RF power repeatedly on the

same point. A relatively new aspect was the electrical characterization of the previously ablated tissue. Section 2.1 addresses this issue and justifies from currently available experimental data the assumptions made in this study.

3. Results

Figure 3 shows the lesion size (depth and maximum width) for different intervals between RF pulses (t_{INT}) and for pulse durations of 20 and 30 s. The dimensions are plotted at four times: just at the end of the first pulse, at the beginning of the second pulse, at the end of the second pulse, and 90 s later. Due to the extra growth of the lesion during the period after the first pulse (caused by thermal latency), growth increases with t_{INT} time. This effect is especially important for short intervals. The opposite effect occurs after the second RF pulse, i.e. the shorter the t_{INT} the larger the lesion size. For instance, in quantitative terms, for two consecutive 20 s pulses separated by a 5 s interval, lesion depth increased from 2.6 mm to 3.0 mm during the interval, reaching 3.9 mm at the end of the second pulse and 4.8 mm after 90 s without RF power. With a 30 s interval, lesion depth increased from 2.6 mm to 3.2 mm during the interval, reaching 3.7 mm at the end of the second pulse and 4.5 mm after 90 s, with similar behavior for the maximum width. To sum up, with two consecutive 20 s pulses, there was a difference of 0.3 mm in depth and 0.5 mm in width between waiting 5 s or 30 s between consecutive RF pulses. The behavior was similar for 30 s pulses, with lesion depth and maximum width of 0.2 mm and 0.4 mm larger, respectively, for an interval of 5 s vs. 30 s.

Figure 4 shows the maximum tissue temperature (T_{MAX}) reached in the tissue for different t_{INT} intervals and for two pulse durations (20 and 30 s). The values are also shown for the four first times mentioned. T_{MAX} was higher at the end of the first 30 s pulse than the 20 s pulse (as

expected, since the energy was 33% higher). T_{MAX} during the second pulse was higher for short t_{INT} intervals, reaching values above 100 ºC with two consecutive 30 s pulses separated by less than 25 s.

Figure 5 shows the temperature distributions in the tissue at different times in consecutive ablations (t_{INT} of 5 and 30 s) and for two pulse durations (20 and 30 s) at three different times: just at the end of the first pulse, at the beginning of the second pulse, and at the end of the second pulse.

Figure 6 shows the lesion depth computed for different times in almost immediate ablations (t_{INT} = 5 s) and for two pulse durations (20 and 30 s). T_{MAX} values are given for the different times. The greater the electrode depth the higher the maximum tissue temperature. The behavior of these two parameters during the sequential application of the pulses was similar for the three insertion depth values.

4. Discussion

4.1. Effect of interval between RF pulses

This simulation study aimed to assess the effect of the interval between two consecutive RF pulses on lesion size and maximum temperature. Repeated application of RF power at adjacent sites has been suggested to ablate extended arrhythmogenic areas in the context of ventricular tachycardia ablation [2]. For instance, Grubman *et al* [24] reported that the delivery of closely spaced lesions using a non-irrigated tipped temperature-controlled catheter (30–60 s, 65 ºC) could produce a confluent lesion significantly larger than those reported using a single pulse. Likewise, temperature-controlled ablation using bipolar surgical forceps has been shown to be safe when RF power is applied twice or even three times on the same site [25]. We think that

while temperature-controlled ablation seems to be safe for repeated pulses, power-controlled ablation (as currently used to treat atrial fibrillation) could cause overheating, since the second RF pulse is applied on pre-heated tissue which is also more conductive (due to the irreversible and reversible changes of the electrical conductivity), which was the reason for our study.

For both 20 s and 30 s pulses, our results show that in general the interval between RF pulses plays an important role in terms of lesion size and T_{MAX}. *In-silico* modeling, unlike experimental and clinical studies, can progressively analyze lesion growth during the sequence of applying the two pulses. We found that the shorter the time between pulses, the smaller the post-RF growth after the first pulse since the second pulse "interrupts" the extra growth caused by thermal latency after cutting off RF power [16,21,26]. However, the almost immediate application of the second pulse encounters a highly preheated substrate (e.g. >60 ºC for t_{INT} = 5 s, see Fig. 4) and therefore more electrically conductive, which means a larger lesion just after the second pulse, reaching considerably higher temperatures than during the first pulse. Even when pulses are applied with a considerable time difference (t_{INT} = 70 s) the substrate on which the second pulse is applied is still warm (~44 ºC), which implies that it is ~10% more conductive due to the reversible change (considering an increase of +1.5%/ºC and a difference between 44 ºC and 37 ºC) and to the irreversible change induced by coagulative necrosis after the first pulse (50% more conductive). Finally, during the 90 s interval after the second pulse, the extra growth is also slightly larger in short intervals, possibly because there is more accumulated heat in the tissue.

The results also show that there is a direct relationship between lesion size and T_{MAX}. The more consecutive the pulses applied, the higher the T_{MAX}, reaching over 100 ºC in the case of two 30 s pulses applied almost in succession (t_{INT} < 20 s, see Fig. 4). T_{MAX} at the beginning of the second pulse is lower at longer intervals. However, after 1 minute this drop is almost negligible.

All the foregoing is a qualitative and physical explanation in electrical and thermal terms.

In quantitative terms, it is important to assess the increase in lesion size due to the application of the second RF pulse, and the associated risk of overheating. If only one RF pulse is applied, lesion depths are 3.4 mm for a 20 s pulse, and 4.1 mm for a 30 s pulse. These values would imply T_{MAX} values of 79.2 ºC and 92.7 ºC, respectively. On the other hand, if a second pulse is applied almost immediately (t_{INT} = 5 s), lesion depths are 4.8 mm for a 20 s pulse, and 5.6 mm for a 30 s pulse, which is an increase of 1.4 mm and 1.5 mm for pulses of 20 s and 30 s, respectively. If the interval between pulses is longer than 30 s, this increase is 1.1 mm and 1.3 mm for 20 s and 30 s pulses, respectively.

Applying a second pulse involves the risk of overheating: while the first 20 s pulse causes a T_{MAX} of 79 ºC, the second implies values ranging from 92 and 96 ºC (the higher temperatures the shorter the interval between pulses), i.e. T_{MAX} is 13–17 ºC higher than when only one pulse is applied. The behavior is similar for 30 s pulses: the first pulse causes a T_{MAX} of 93 ºC, while the second implies values ranging from 98 to 104 ºC, i.e. T_{MAX} is 6–11 ºC higher than when only one pulse is applied. This difference between the two pulse durations could be even higher, considering that we really evaluated the T_{MAX} value just at the end of the pulse and that it increases slightly more during post-RF in 20 s than in 30 s pulses [26].

Finally, as shown in Fig. 6, the evolution of lesion depth and maximum tissue temperature during the sequential application of the pulses is very similar for the range of insertion depths between 0.25 and 0.75 mm. As expected, both lesion depths and maximum tissue temperatures are greater the higher the insertion depth, since there is more contact surface between electrode and tissue and more power is targeted towards the tissue.

4.2. Clinical implications

The results suggest that two moderately long pulses (20–30 s) on the same ablation point could increase lesion depth by 1.1–1.5 mm more than a single pulse. Although this could suggest better ablation efficiency, the edema effect of RF heating (e.g. found by Wright *et al* [27]) should also be taken into account. This phenomenon thickens the cardiac wall by about 25% [27,28] (although other authors have reported much higher values of around 400% [29]). No computational model has so far included this phenomenon, possibly due to the lack of experimental data on the composition of the edematous zone induced by RF ablation. We could hypothesize that if edema induces thickening within the first few seconds and normally disappears after 4 weeks [29], the chronic lesion could be shallower than the acute lesion by a similar percentage to the tissue thickening (~25%). In fact, edema should be taken into account in any RF cardiac ablation computer model and not only in the context of studying repetitive applications. In the context of the present study, if repetitive applications are aimed at increasing lesion depth, edema could be critical when assessing ablation efficacy, particularly when the computed lesion depth is compared to the thickness of the atrial wall (in AF ablation) or the depth of the target zone (in VT ablation). Our results suggest a higher overheating risk (T_{MAX}) when the pulses are more consecutive, which could be counterproductive if thickening is directly related to the maximum temperature reached.

To sum up, our results suggest that there is a delicate balance in deciding whether or not to apply a second pulse, and between long or short intervals between consecutive pulses. It also seems that pulse duration is relevant in this equilibrium; for example, two 20 s almost consecutive pulses (5 s interval) create a 4.8 mm deep lesion with a maximum temperature of 96 ^{o}C, while a single longer pulse (30 s) creates a 4.1 mm deep lesion with a maximum tissue

temperature of 93 ºC. With these values it is difficult to decide which is the most suitable, applying a long pulse or several short ones at the same point, especially given the current uncertainty about the relationship between the second RF pulse and greater edema-induced thickening of the tissue.

All the comments up to now concern maximizing lesion depth. Although we considered that the pulses were applied exactly at the same site (to obtain a two-dimensional model and reduce computational requirements), it seems reasonable to extend the conclusions to two RF pulses very close together when lesions can be partially overlapped. Our results suggest that the irreversible change in electrical conductivity of a previously ablated zone could seriously alter the geometry of nearby lesions, i.e. electrophysiologists who perform a point-to-point lesion line should not think that they are creating independent lesions on an "intact" substrate, but rather are ablating more conductive tissue as the overlap is greater and the shorter the interval between pulses. In practical terms, our results suggest that when ablating a thin atrial wall in which an effective lesion has already been possibly achieved by a single pulse, the new pulse in the same vicinity should allow the longest possible time between pulses (e.g. 1 min) to minimize the risk of overheating, and possibly also the edema-induced tissue thickening. In this regard, in the context of atrial fibrillation ablation, it has been recently suggested that the sufficient time between applications must be allowed to avoid temperature stacking which could cause damage to the esophagus [30].

Considering the computer results and the physical explanation based on the changes in electrical conductivity after the first pulse, we now propose to explore the combination of a first RF pulse at constant power and a second at constant temperature. This would make sense, since constant temperature ablation modulates the applied power according to tissue conductivity to

keep electrode temperature constant, thus compensating for any excess power and avoiding overheating [24]. Future experimental studies should assess whether these combined modes enlarge the lesion applying pulses at the same point.

4.3. Limitations of the study

The study has certain limitations regarding the specific conditions considered and the methods used to model some phenomena. We only considered a perpendicular catheter, which means that the values of lesion size and T_{MAX} obtained could be different in other circumstances. The insertion of the electrode was assumed to be sharp (i.e. an elastic model was not considered). This approach slightly overestimates the percentage of electrode surface in contact with the tissue and so tends to overestimate lesion size and tissue temperature [31]. We only considered low blood flow condition around the electrode (as occurring in ablations sites associated with patients with chronic atrial fibrillation and dilated atria). Since it is known that blood flow can affect the lesion size and tissue temperature, other results could be obtained in case of high blood flow as occurring e.g. just above the mitral valve [32]. However, although the values predicted by the simulations could be different than those under other specific conditions, the conclusions on the effect of the second pulse and the interval between pulses should remain valid.

Also, the repeated application of RF pulses assumed no loss of contact between electrode and tissue surface. In a real clinical situation, the electrode could lose contact after the first pulse before re-contacting for the second. The only difference with what we modeled is in the heat evacuation in the interval between pulses, either through the electrode itself and from there to the circulating blood or directly through the circulating blood. We think that this difference will not have a significant impact on the conclusions. The model did not consider the heartbeat-induced

electrode displacement since a previous modeling study showed very similar in terms of lesion size and temperature to those obtained with a static model [33].

Regarding the methods of modeling some phenomena, our *in-silico* model did not solve the velocity distribution in the blood, but its thermal effect was modeled by the heat transfer coefficient on the blood-electrode and blood-myocardium interfaces. This approach predicts lesion depth reasonably well but overestimates the surface width. The Discussion and Conclusions were thus stated in terms of lesion depth. On the other hand, only irreversible changes in electrical conductivity were considered since the experimental data suggest that heat-induced irreversible change of other tissue properties (e.g. thermal conductivity) is less important [34]. Finally, it is important to emphasize that the electrical conductivity of the myocardium and its thermal dependence were taken from kidney and extrapolated from 78 ºC [4], due to the lack of experimental data for myocardium and temperatures reaching 100 ºC. Despite these limitations the results are physically consistent in qualitative terms and encourage us to do further experimental studies to quantify the benefits and risks of applying consecutive constant power pulses at the same point, overlapping lesions, or exploring other methods of enlarging lesion size while avoiding overheating.

5. Conclusions

Our results suggest that applying a second RF pulse at the same ablation site might increase lesion depth by 1–1.5 mm more than a single pulse but may also lead to more overheating (up to 17 ºC more than with a single pulse). Both the lesion depth and maximum temperature become greater as the interval between pulses is reduced. It should be taken into account that the absolute values of lesion increase and maximum temperature depend a lot on the changes in the electrical

conductivity of the myocardium during RF heating, which has not yet been well characterized experimentally.

References

1. Barkagan M, Contreras-Valdes FM, Leshem E, Buxton AE, Nakagawa H, Anter E. High-power and short-duration ablation for pulmonary vein isolation: Safety, efficacy, and long-term durability. J Cardiovasc Electrophysiol. 2018 Sep;29(9):1287-1296. doi: 10.1111/jce.13651.
2. Simmers TA, Wittkampf FH, Hauer RN, Robles de Medina EO. In vivo ventricular lesion growth in radiofrequency catheter ablation. Pacing Clin Electrophysiol. 1994 Mar;17(3 Pt 2):523-31. doi: 10.1111/j.1540-8159.1994.tb01421.x.
3. Ring ME, Huang SK, Gorman G, Graham AR. Determinants of impedance rise during catheter ablation of bovine myocardium with radiofrequency energy. Pacing Clin Electrophysiol. 1989 Sep;12(9):1502-13. doi: 10.1111/j.1540-8159.1989.tb06155.x.
4. Pop M, Molckovsky A, Chin L, Kolios MC, Jewett MA, Sherar MD. Changes in dielectric properties at 460 kHz of kidney and fat during heating: importance for radio-frequency thermal therapy. Phys Med Biol. 2003 Aug 7;48(15):2509-25. doi: 10.1088/0031-9155/48/15/317.
5. Andreozzi A, Brunese L, Iasiello M, Tucci C, Vanoli GP. Numerical analysis of the pulsating heat source effects in a tumor tissue. Comput Methods Programs Biomed. 2021 Mar;200:105887. doi: 10.1016/j.cmpb.2020.105887.
6. González-Suárez A, Pérez JJ, Irastorza RM, D'Avila A, Berjano E. Computer modeling of radiofrequency cardiac ablation: 30 years of bioengineering research. Comput Methods Programs Biomed. 2021 Nov 18:106546. doi: 10.1016/j.cmpb.2021.106546.
7. Nath S, Redick JA, Whayne JG, Haines DE. Ultrastructural observations in the myocardium beyond the region of acute coagulation necrosis following radiofrequency catheter ablation. J Cardiovasc Electrophysiol. 1994 Oct;5(10):838-45. doi: 10.1111/j.1540-8167.1994.tb01122.x.
8. Sulkin MS, Laughner JI, Hilbert S, Kapa S, Kosiuk J, Younan P, Romero I, Shuros A, Hamann JJ, Hindricks G, Bollmann A. Novel Measure of Local Impedance Predicts Catheter-Tissue Contact and Lesion Formation. Circ Arrhythm Electrophysiol. 2018 Apr;11(4):e005831. doi: 10.1161/CIRCEP.117.005831.
9. Salazar Y, Bragos R, Casas O, Cinca J, Rosell J. Transmural versus nontransmural in situ electrical impedance spectrum for healthy, ischemic, and healed myocardium. IEEE Trans Biomed Eng. 2004 Aug;51(8):1421-7. doi: 10.1109/TBME.2004.828030.
10. Schwartzman D, Chang I, Michele JJ, Mirotznik MS, Foster KR. Electrical impedance properties of normal and chronically infarcted left ventricular myocardium. J Interv Card Electrophysiol. 1999 Oct;3(3):213-24. doi: 10.1023/a:1009887306055.
11. Hasgall PA, Di Gennaro F, Baumgartner C, et al, "IT'IS Database for thermal and electromagnetic parameters of biological tissues," Version 4.0, May 15, 2018, DOI: 10.13099/VIP21000-04-0. itis.swiss/database.
12. Castro-López DL, Trujillo M, Berjano E, Romero-Mendez R. Two-compartment mathematical modeling in RF tumor ablation: New insight when irreversible changes in electrical conductivity are considered. Math Biosci Eng. 2020 Nov 11;17(6):7980-7993. doi: 10.3934/mbe.2020405.
13. Yan S, Gu K, Wu X, et al. Computer simulation study on the effect of electrode-tissue contact force on thermal lesion size in cardiac radiofrequency ablation. Int J Hyperthermia. 2020;37(1):37-48. doi: 10.1080/02656736.2019.1708482.
14. Deneke T, Nentwich K, Berkovitz A, et al. High-resolution infrared thermal imaging of the esophagus during atrial fibrillation ablation as a predictor of endoscopically detected thermal lesions: results from the HEAT-AF study. Circ Arrhythm Electrophysiol. 2018 Nov;11(11):e006681. doi: 10.1161/CIRCEP.118.006681.
15. Irastorza RM, Gonzalez-Suarez A, Pérez JJ, et al. Differences in applied electrical power between full thorax models and limited-domain models for RF cardiac ablation. Int J Hyperthermia. 2020;37(1):677-687. doi: 10.1080/02656736.2020.1777330.
16. Irastorza RM, d'Avila A, Berjano E. Thermal latency adds to lesion depth after application of high-power short-duration radiofrequency energy: Results of a computer-modeling study. J Cardiovasc Electrophysiol.

2018 Feb;29(2):322-327. doi: 10.1111/jce.13363.
17. Berjano EJ. Theoretical modeling for radiofrequency ablation: state-of-the-art and challenges for the future. Biomed Eng Online. 2006 Apr 18;5:24. doi: 10.1186/1475-925X-5-24.
18. Abraham JP, Sparrow EM. A thermal-ablation bioheat model including liquid-to-vapor phase change, pressure- and necrosis-dependent perfusion, and moisture-dependent properties. Int J Heat Mass Tran. 2007; 50(13-14):2537-2544.
19. Pérez JJ, Ewertowska E, Berjano E. Computer modeling for radiofrequency bipolar ablation inside ducts and vessels: relation between pullback speed and impedance progress. Lasers Surg Med. 2020 Nov;52(9):897-906. doi: 10.1002/lsm.23230.
20. González-Suárez A, Berjano E. Comparative analysis of different methods of modeling the thermal effect of circulating blood flow during RF cardiac ablation. IEEE Trans Biomed Eng. 2016 Feb;63(2):250-9.
21. Nakagawa H, Ikeda A, Sharma T, Govari A, Ashton J, Maffre J, Lifshitz A, Fuimaono K, Yokoyama K, Wittkampf FHM, Jackman WM. Comparison of In Vivo Tissue Temperature Profile and Lesion Geometry for Radiofrequency Ablation With High Power-Short Duration and Moderate Power-Moderate Duration: Effects of Thermal Latency and Contact Force on Lesion Formation. Circ Arrhythm Electrophysiol. 2021 Jul;14(7):e009899. doi: 10.1161/CIRCEP.121.009899.
22. González-Suárez A, Pérez JJ, Berjano E. Should fluid dynamics be included in computer models of RF cardiac ablation by irrigated-tip electrodes? Biomed Eng Online. 2018 Apr 20;17(1):43.
23. Babuska I, Tinsley Oden J. Verification and validation in computational engineering and science: basic concepts. Comput. Methods Appl. Mech. Engrg. 2004:193:4057–4066. doi:10.1016/j.cma.2004.03.002.
24. Grubman E, Pavri BB, Lyle S, Reynolds C, Denofrio D, Kocovic DZ. Histopathologic effects of radiofrequency catheter ablation in previously infarcted human myocardium. J Cardiovasc Electrophysiol. 1999 Mar;10(3):336-42. doi: 10.1111/j.1540-8167.1999.tb00680.x.
25. Wakasa S, Kubota S, Shingu Y, Kato H, Ooka T, Tachibana T, Matsui Y. Histological assessment of transmurality after repeated radiofrequency ablation of the left atrial wall. Gen Thorac Cardiovasc Surg. 2014 Jul;62(7):428-33. doi: 10.1007/s11748-013-0363-9..
26. Pérez JJ, González-Suárez A, Maher T, Nakagawa H, d'Avila A, Berjano E. Relationship between luminal esophageal temperature and volume of esophageal injury during RF ablation: In silico study comparing low power-moderate duration vs. high power-short duration. J Cardiovasc Electrophysiol. 2021 Dec 2. doi: 10.1111/jce.15311.
27. Wright M, Harks E, Deladi S, Fokkenrood S, Brink R, Belt H, Kolen AF, Rankin D, Stoffregen W, Cockayne DA, Cefalu J, Haines DE. Characteristics of Radiofrequency Catheter Ablation Lesion Formation in Real Time In Vivo Using Near Field Ultrasound Imaging. JACC Clin Electrophysiol. 2018 Aug;4(8):1062-1072. doi: 10.1016/j.jacep.2018.04.002.
28. Gao X, Chang D, Bilchick KC, Hussain SK, Petru J, Skoda J, Sediva L, Neuzil P, Mangrum JM. Left atrial thickness and acute thermal injury in patients undergoing ablation for atrial fibrillation: Laser versus radiofrequency energies. J Cardiovasc Electrophysiol. 2021 May;32(5):1259-1267. doi: 10.1111/jce.15011.
29. Schwartzman D, Ren JF, Devine WA, Callans DJ. Cardiac swelling associated with linear radiofrequency ablation in the atrium. J Interv Card Electrophysiol. 2001 Jun;5(2):159-66. doi: 10.1023/a:1011477408021.
30. Yavin HD, Bubar ZP, Higuchi K, Sroubek J, Kanj M, Cantillon D, Saliba WI, Tarakji KG, Hussein AA, Wazni O, Anter E. Impact of High-Power Short-Duration Radiofrequency Ablation on Esophageal Temperature Dynamic. Circ Arrhythm Electrophysiol. 2021 Oct 28:CIRCEP121010205. doi: 10.1161/CIRCEP.121.010205. Epub ahead of print.
31. Petras A, Leoni M, Guerra JM, Jansson J, Gerardo-Giorda L. A computational model of open-irrigated radiofrequency catheter ablation accounting for mechanical properties of the cardiac tissue. Int J Numer Method Biomed Eng. 2019 Nov;35(11):e3232. doi: 10.1002/cnm.3232.
32. Tungjitkusolmun S, Vorperian VR, Bhavaraju N, Cao H, Tsai JZ, Webster JG. Guidelines for predicting lesion size at common endocardial locations during radio-frequency ablation. IEEE Trans Biomed Eng. 2001 Feb;48(2):194-201. doi: 10.1109/10.909640.
33. Pérez JJ, Nadal E, Berjano E, González-Suárez A. Computer modeling of radiofrequency cardiac ablation including heartbeat-induced electrode displacement. Comput Biol Med. 2022 Feb 25;144:105346. doi: 10.1016/j.compbiomed.2022.105346.
34. Bhattacharya A, Mahajan RL. Temperature dependence of thermal conductivity of biological tissues. Physiol Meas. 2003 Aug;24(3):769-83. doi: 10.1088/0967-3334/24/3/312.

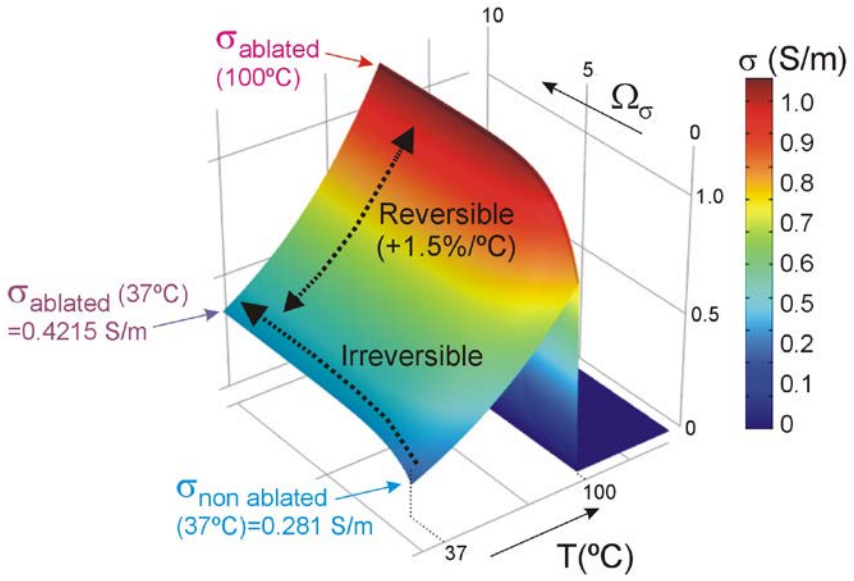

Figure 1 Reversible and irreversible changes of electrical conductivity (σ) of the myocardium.

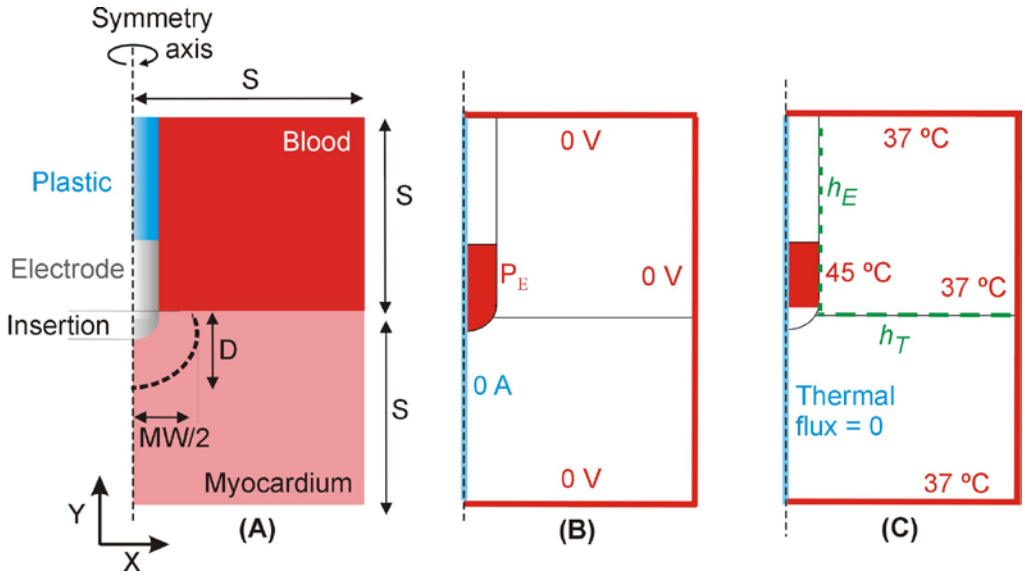

Figure 2 **A:** Geometry of the two-dimensional computational model built (not to scale) including an ablation electrode (8 Fr, 3.5 mm) inserted into a fragment of myocardium and completely surrounded by blood. Dimension of myocardium and blood (S) is obtained from a convergence test. Lesion size is computed using the depth (D) and maximum width (MW). **B:** Electrical boundary conditions. **C:** Thermal boundary conditions. h_E and h_T are the thermal convection coefficients at the electrode–blood and tissue–blood interfaces, respectively.

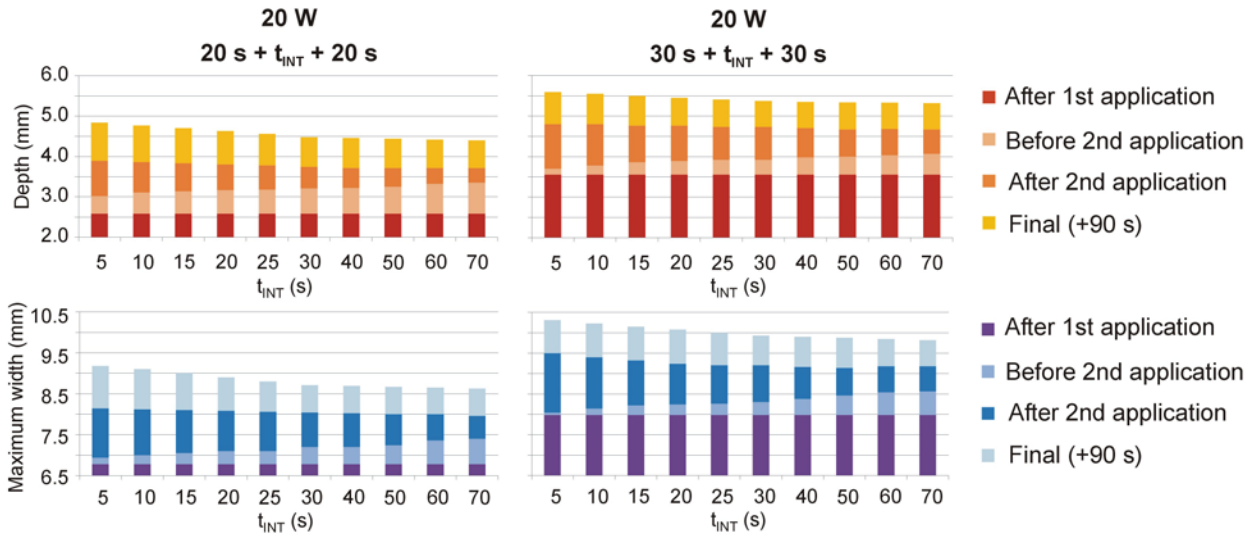

Figure 3 Lesion sizes (depth and maximum width) for different time intervals between RF ablations (t_{INT}) and for two pulses durations: 20 s (left) and 30 s (right). The colors illustrate how the lesion grows at four consecutive moments: just after the first pulse is finished, when the second pulse begins, when the second pulse ends, and 90 s later.

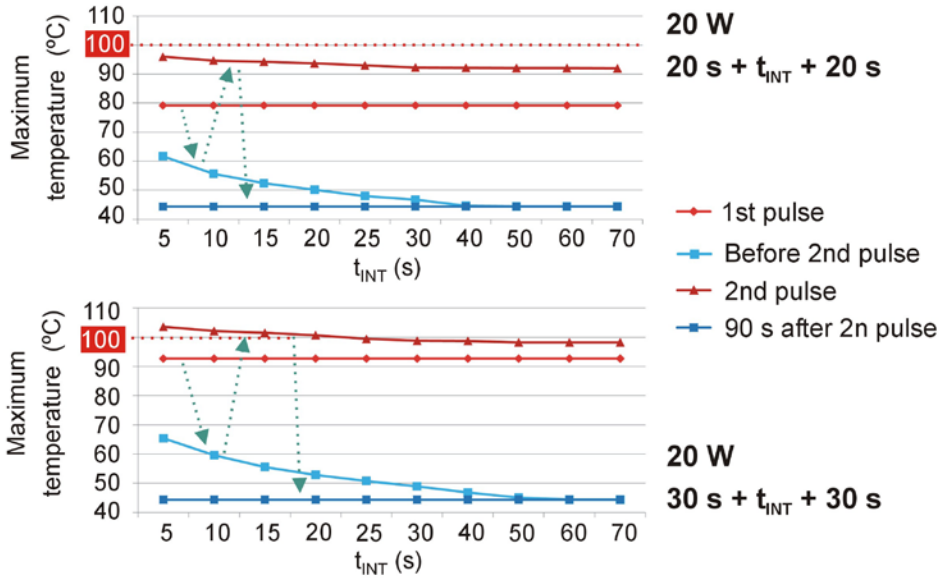

Figure 4 Maximum temperature reached in the tissue for different time intervals between RF ablations (t_{INT}) and for two pulse durations: 20 s (top) and 30 s (bottom). The values are also shown at four consecutive times: just after the first pulse is ended, when the second pulse begins, when the second pulse ends, and 90 s later. Green dotted lines indicate the sequence of the maximum temperatures for these four instants. Red dotted line gives the 100 ºC value suggesting overheating and risk of steam pop.

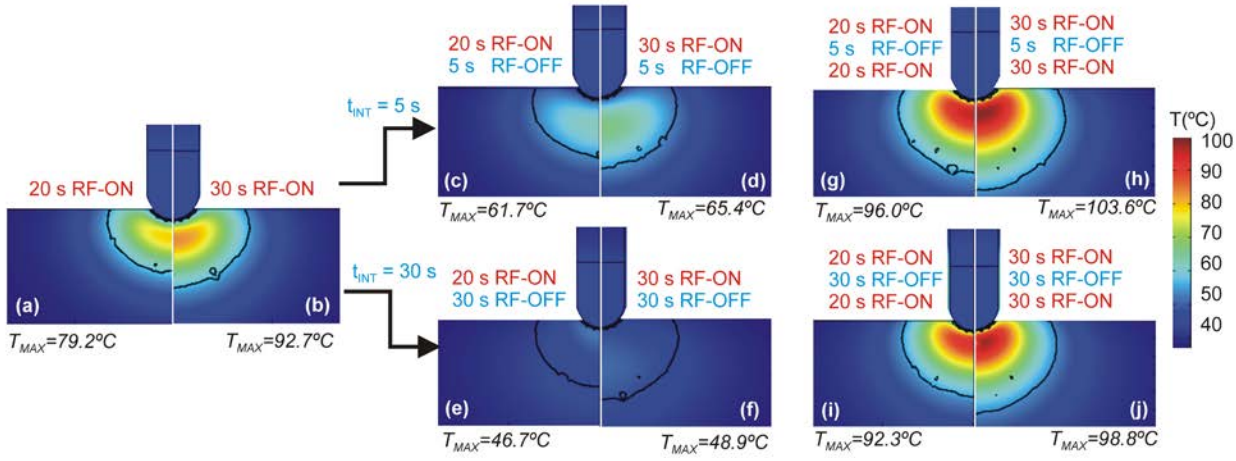

Figure 5 Temperature distributions in the tissue for three different time intervals between RF ablations t_{INT} (5 and 30 s) and for two pulse durations (20 and 30 s). The plots are those of three times: just at the end of the first pulse (**a,b**), at the beginning of the second pulse (**c-f**), at the end of the second pulse (**g-j**). Black solid line represents the lesion contour.

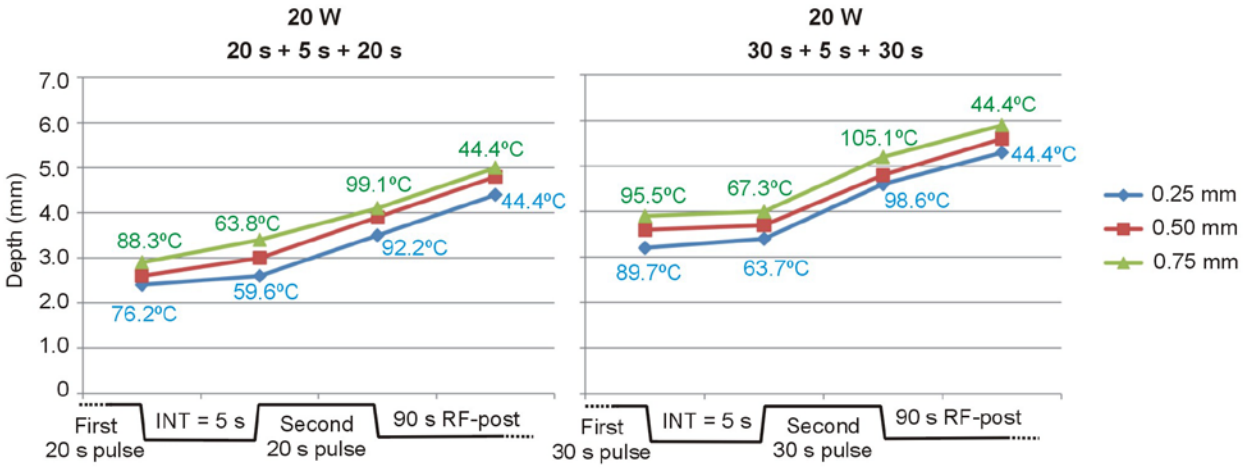

Figure 6 Lesion depth computed for different electrode insertion depths into the tissue (0.25, 0.5 and 0.75 mm) at different times over two almost immediate RF pulses (t_{INT} = 5 s) and for 20 and 30 s pulse durations. The maximum temperature values reached in the tissue at each time are indicated for 0.25 and 0.75 mm (note that the 0.5 mm values are shown on the plots in Fig. 5).